GENETICS

Modulation of mtDNA copy number ameliorates the pathological consequences of a heteroplasmic mtDNA mutation in the mouse

R. Filograna[1,2], C. Koolmeister[1,2], M. Upadhyay[1,2], A. Pajak[1,2], P. Clemente[1,2], R. Wibom[3], M. L. Simard[4], A. Wredenberg[1,2,3], C. Freyer[1,2,3], J. B. Stewart[4], N. G. Larsson[1,2,3,4]*

Heteroplasmic mtDNA mutations typically act in a recessive way and cause mitochondrial disease only if present above a certain threshold level. We have experimentally investigated to what extent the absolute levels of wild-type (WT) mtDNA influence disease manifestations by manipulating TFAM levels in mice with a heteroplasmic mtDNA mutation in the $tRNA^{Ala}$ gene. Increase of total mtDNA levels ameliorated pathology in multiple tissues, although the levels of heteroplasmy remained the same. A reduction in mtDNA levels worsened the phenotype in postmitotic tissues, such as heart, whereas there was an unexpected beneficial effect in rapidly proliferating tissues, such as colon, because of enhanced clonal expansion and selective elimination of mutated mtDNA. The absolute levels of WT mtDNA are thus an important determinant of the pathological manifestations, suggesting that pharmacological or gene therapy approaches to selectively increase mtDNA copy number provide a potential treatment strategy for human mtDNA mutation disease.

INTRODUCTION

Mitochondria are highly dynamic double-membrane organelles present in almost all eukaryotic cells. According to recent data, at least 1158 different proteins are localized in mammalian mitochondria to ensure a variety of metabolic functions of the organelle (*1*). The primary mitochondrial role is to satisfy most of the cellular energy demand by producing adenosine 5′-triphosphate (ATP) through oxidative phosphorylation (OXPHOS). Mitochondria carry their own genome [mitochondrial DNA (mtDNA)], which is a double-stranded circular molecule, that in mammals contain 37 genes encoding 13 structural subunits of the OXPHOS machinery and all RNA components needed for mitochondrial translation, i.e., 12*S* ribosomal RNA (rRNA), 16*S* rRNA, and a set of 22 transfer RNAs (tRNAs) (*2*). Most of the mitochondrial proteins are thus encoded in the nucleus, synthesized in the cytoplasm, and imported into mitochondria. The dual genetic control of the biogenesis of mitochondria means that important enzymatic machineries, such as the mitochondrial ribosomes and the OXPHOS protein complexes, contain critical components encoded by both mtDNA and nuclear genes. An unexpected large proportion of the nucleus-encoded mitochondrial proteome (~25%) is devoted to the maintenance of mtDNA and regulation of its gene expression (*3*).

Mutations of either mtDNA or nuclear genes are important causes of mitochondrial diseases with impaired OXPHOS function (*4*). These genetic disorders are often multisystemic and typically involve organs highly dependent on aerobic respiration (*5*). Mitochondrial dysfunction has also been implicated in numerous common age-related pathologies, which include neurodegenerative diseases, cardiovascular disorders, diabetes, obesity, and cancer, as well as in the naturally occurring aging process (*6*). Despite the substantial advances in our knowledge of pathophysiological mechanisms underlying mitochondrial diseases, effective treatments are still lacking, and clinical management of these devastating conditions remains mostly symptomatic (*7*).

Epidemiological studies have estimated that at least 1:5000 of the population is affected by pathogenic mtDNA mutations (*8*). There are multiple copies of mtDNA in every cell, and this polyploidy makes mitochondrial genetics different from Mendelian genetics. mtDNA is exclusively maternally inherited and subject to segregation and purifying selection in the germ line (*9*). The vast majority of pathogenic mtDNA mutations are heteroplasmic and are therefore only present in a proportion of all mtDNA molecules. Mutant and wild-type (WT) mitochondrial genotypes can thus coexist, and affected cells will only manifest metabolic defects when the mtDNA mutation levels exceed a critical threshold (*10*). In a given tissue, there are frequently mosaic patterns where only a subset of cells is OXPHOS deficient. Although our current understanding of the threshold effect is limited, it has been previously observed that the threshold can vary from mutation to mutation, from organ to organ, and between different family members (*11*). Over the course of an individual's life, the level of heteroplasmy can shift either up or down as consequence of genetic drift and selection. The explanation for these phenomena is that the replication of mtDNA occurs continuously during the cell cycle, and the mutated and WT mtDNA molecules are unevenly transmitted and vary markedly between daughter cells. In dividing tissues, there is also the possibility of selection against mutated mtDNA over time, leading to cell clones with lower mutation levels (*10*), e.g., as observed in blood from human patients with point mutations or deletions of mtDNA (*12*, *13*).

Correlative data from human patients suggest that the total mtDNA copy number may influence to what extent a given level of a heteroplasmic mtDNA mutation is pathogenic (*14*). However, critical experimental tests of the role for mtDNA copy number as a determinant of the pathogenicity of a specified heteroplasmic mtDNA mutation are still lacking. To this end, we used mice carrying the heteroplasmic m.5024C > T mutation in the mitochondrial tRNA alanine ($tRNA^{Ala}$) gene (henceforth denoted "C5024T mice"), which

[1]Division of Molecular Metabolism, Department of Medical Biochemistry and Biophysics, Karolinska Institutet, S-171 76 Stockholm, Sweden. [2]Max Planck Institute Biology of Ageing - Karolinska Institutet Laboratory, Karolinska Institutet, S-171 77 Stockholm, Sweden. [3]Center for Inherited Metabolic Diseases, Karolinska University Hospital, S-171 76 Stockholm, Sweden. [4]Department of Mitochondrial Biology, Max Planck Institute for Biology of Ageing, D-50931 Cologne, Germany.
*Corresponding author. Email: nils-goran.larsson@ki.se

recapitulate many features of human mitochondrial disease, develop a mild progressive cardiomyopathy and cytochrome *c* oxidase (COX) deficiency in many organs, and also show selection against mutated mtDNA in proliferating tissues (*15*). Because the C5024T mice only have a single pathogenic mtDNA mutation, the influence of mtDNA copy number on genotype-phenotype correlations can be studied at high resolution. We show here that C5024T mice exhibit a robust increase in mtDNA levels with age, consistent with an endogenous mechanism that counteracts the mitochondrial dysfunction caused by heteroplasmic mtDNA mutations. We experimentally manipulated mtDNA levels by either increasing or decreasing the expression of the mitochondrial transcription factor A (TFAM) in C5024T mice. TFAM is essential for packaging mtDNA into mitochondrial nucleoids (*16*) and is also necessary for mtDNA transcription initiation (*17*). A direct role for TFAM in mtDNA copy number regulation has been established both in vitro (*18*) and in vivo (*19*, *20*). Heterozygous *Tfam* knockout mice have ~50% decrease in mtDNA levels (*19*), whereas moderate overexpression of *Tfam* results in ~50% increase of mtDNA copy number (*20*). The series of experiments we present here show that mtDNA copy number manipulation has a crucial impact on the phenotype of C5024T mice. The effects vary among tissues and strongly depend on their proliferative capacity.

RESULTS

Mice harboring the C5024T mutation have increased mtDNA copy number

The heteroplasmic C5024T mutation of the $tRNA^{Ala}$ gene (Fig. 1A) leads to impaired mitochondrial translation if present at high levels (*15*). However, it is unclear to what extent the interplay between the proportion of mutated mtDNA (i.e., level of heteroplasmy) and total mtDNA copy number influences pathophysiology. To address this issue, we measured mtDNA copy number in mice carrying different levels of the C5024T mutation at early and late disease stages using quantitative polymerase chain reaction (qPCR) analyses of DNA extracted from colon and heart. At 20 weeks of age, the mutant mice had normal mtDNA levels in both tissues as determined by two different probes (Fig. 1B and fig. S1A). In contrast, at 50 weeks of age, when the animals are symptomatic (*15*), the mtDNA copy number was increased ~1.4- to 1.7-fold in colon and ~1.8- to 2-fold in the heart. In older animals, the increase in mtDNA copy number was more pronounced at high mutation levels in the colon, whereas no such mutation level–dependent effect was seen in the heart (Fig. 1B and fig. S1A). These observations show that mtDNA copy number is increased in C5024T mice at advanced disease stages, likely as a compensatory response induced by the mitochondrial dysfunction.

TFAM overexpression increases the tolerance for high C5024T mutation levels

We proceeded to investigate whether manipulation of mtDNA copy number would affect the maximally tolerated mutation levels transmitted to newborn pups from C5024T mothers. We performed crosses (fig. S1B) to increase mtDNA copy number using bacterial artificial chromosome (BAC) transgenic mice overexpressing mouse TFAM ($Tfam^{+/OE}$) (*21*) and to decrease mtDNA copy number using heterozygous *Tfam* knockout mice ($Tfam^{+/KO}$) (*20*). We analyzed the mutation levels in more than 2000 pups generated from females harboring the C5024T mutation together with normal, high, or low mtDNA copy number (Fig. 1C). The maximally tolerated mutation levels in offspring to C5024T females with normal mtDNA copy number were 80 to 81% (Fig. 1C), which is in good agreement with a previous characterization of this mouse strain (*15*). Overexpression of TFAM in the mother shifted the threshold level for tolerated heteroplasmy in the offspring up to 84% C5024T mutation, whereas reduced expression of TFAM had no effect (Fig. 1C and fig. S1C). These results show that the maximally tolerated proportion of the pathogenic C5024T mutation that can be transmitted through the germ line is increased in mice with high mtDNA copy number.

Manipulation of mtDNA levels in adult mice harboring the C5024T mutation

Next, we performed crosses (fig. S1B) to determine whether experimental modulation of mtDNA copy number would influence the phenotype of adult C5024T mice. Western blot analyses of total tissue extracts from colon and heart revealed that TFAM protein levels were increased by ~50% in the $Tfam^{+/OE}$ and $Tfam^{+/OE}$ C5024T mice, whereas the levels were decreased by ~50% in the $Tfam^{+/KO}$ and $Tfam^{+/KO}$ C5024T mice (Fig. 1D). At 20 weeks of age, there was no difference in mtDNA copy number in the heart or colon between WT and C5024T mice as determined by two different mitochondrial probes (Fig. 1E and fig. S1D). Altered TFAM expression influenced mtDNA copy number to the same extent in mice harboring either WT or C5024T mtDNA and led to a ~1.7-fold increase in $Tfam^{+/OE}$ mice and ~40 to 50% decrease in $Tfam^{+/KO}$ mice (Fig. 1E and fig. S1D). At 50 weeks of age, the mtDNA copy number of C5024T mice was increased ~1.6- to 1.8-fold in the heart and colon in comparison with the levels in age-matched controls (Fig. 1F and fig. S1E). Increased TFAM expression led to an additional increase with ~2.1- to 2.8-fold higher mtDNA levels in $Tfam^{+/OE}$ C5024T mice in both heart and colon (Fig. 1F and fig. S1E). The endogenous response increasing mtDNA copy number in C5024T mice led to almost normal mtDNA levels in $Tfam^{+/KO}$ C5024T mice at the age of 50 weeks in both analyzed tissues (Fig. 1F and fig. S1E). These results show that increased TFAM expression increases mtDNA copy number in mice with both WT and C5024T mutation mtDNA and that the endogenous increase in mtDNA copy number in old C5024T mice is enhanced by TFAM overexpression.

Increased mtDNA levels partially rescue cardiomyopathy and COX deficiency

We continued by investigating how mtDNA copy number affects the pathological manifestations caused by the C5024T mutation, i.e., cardiomyopathy and COX deficiency in different tissues (*15*). At 50 weeks of age, male C5024T mice showed an increased heart-to-body weight ratio in comparison to WT controls (Fig. 2A). Furthermore, the C5024T animals showed an increased expression of molecular markers of cardiomyopathy such as the atrial natriuretic factor (ANF) and the activating transcription factor 5 (ATF5) (Fig. 2B), whereas the expression levels of the ATF4 were unaltered (fig. S1F). These changes were partially ameliorated by TFAM overexpression, whereas reduced TFAM expression exacerbated the heart-to-body weight ratio increase (Fig. 2A).

We used histochemistry of fresh-frozen tissues from 20-, 50-, and 75-week-old mice to assess COX and succinate dehydrogenase (SDH) enzyme activities (Fig. 2, C and D, and fig. S2, A and E). With COX/SDH double staining, cells with normal COX and SDH activities appear brown, whereas cells with COX deficiency appear blue. No or very few blue cells were detected in different tissues from

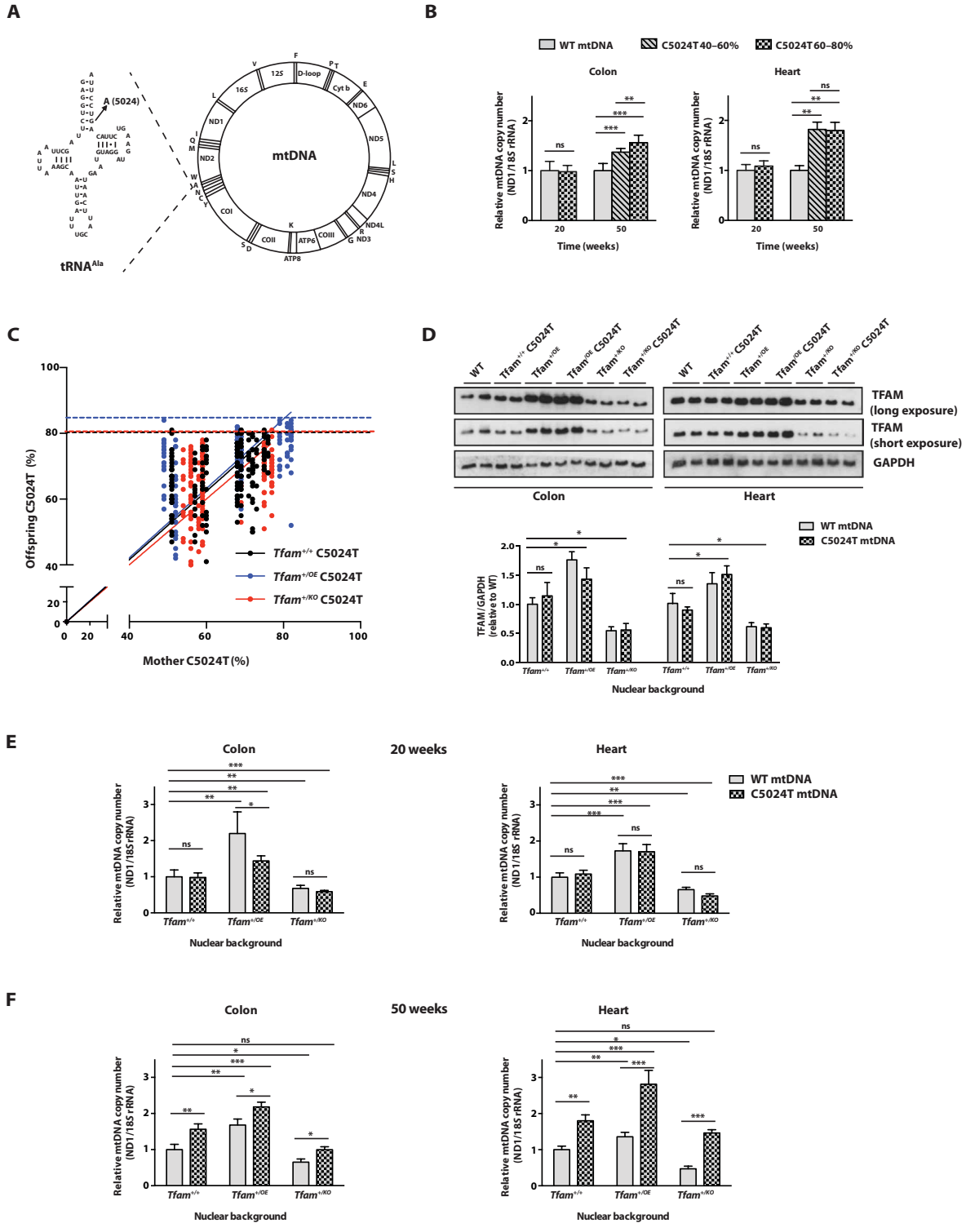

Fig. 1. Germ line transmission of the C5024T mutation and mtDNA copy number manipulation. (**A**) Schematic representation of mouse mtDNA and the structure of the mutated $tRNA^{Ala}$ with a pathogenic mutation in the aminoacyl acceptor stem. (**B**) Quantification of mtDNA copy number by qPCR analysis (ND1/18*S* rRNA) of colon and heart from WT and C5024T mice at the age of 20 and 50 weeks. Data are represented as means ± SEM; $n > 6$. (**C**) Comparison of the levels of the C5024T mutation in offspring ($n = 433$) to heteroplasmic mothers ($n = 28$) measured in ear clips obtained at the age of 3 weeks. The dashed lines represent the maximum observed level of the mutation in the different mouse lines. (**D**) Western blot analysis of TFAM protein levels normalized to GAPDH (glyceraldehyde-3-phosphate dehydrogenase) in colon and heart of mice with different genotypes at the age of 20 weeks. Data are represented as means ± SEM; $n > 5$. (**E** and **F**) Quantification of mtDNA copy number by qPCR (ND1/18*S* rRNA) in heart and colon at 20 (E) and 50 weeks of age (F). Animals with harboring WT or C5024T mtDNA combined with the $Tfam^{+/+}$, $Tfam^{+/OE}$, or the $Tfam^{+/KO}$ alleles were analyzed. Data are represented as means ± SEM; $^{*}P < 0.05$; $^{**}P < 0.01$; $^{***}P < 0.001$; ns, nonsignificant; $n > 6$.

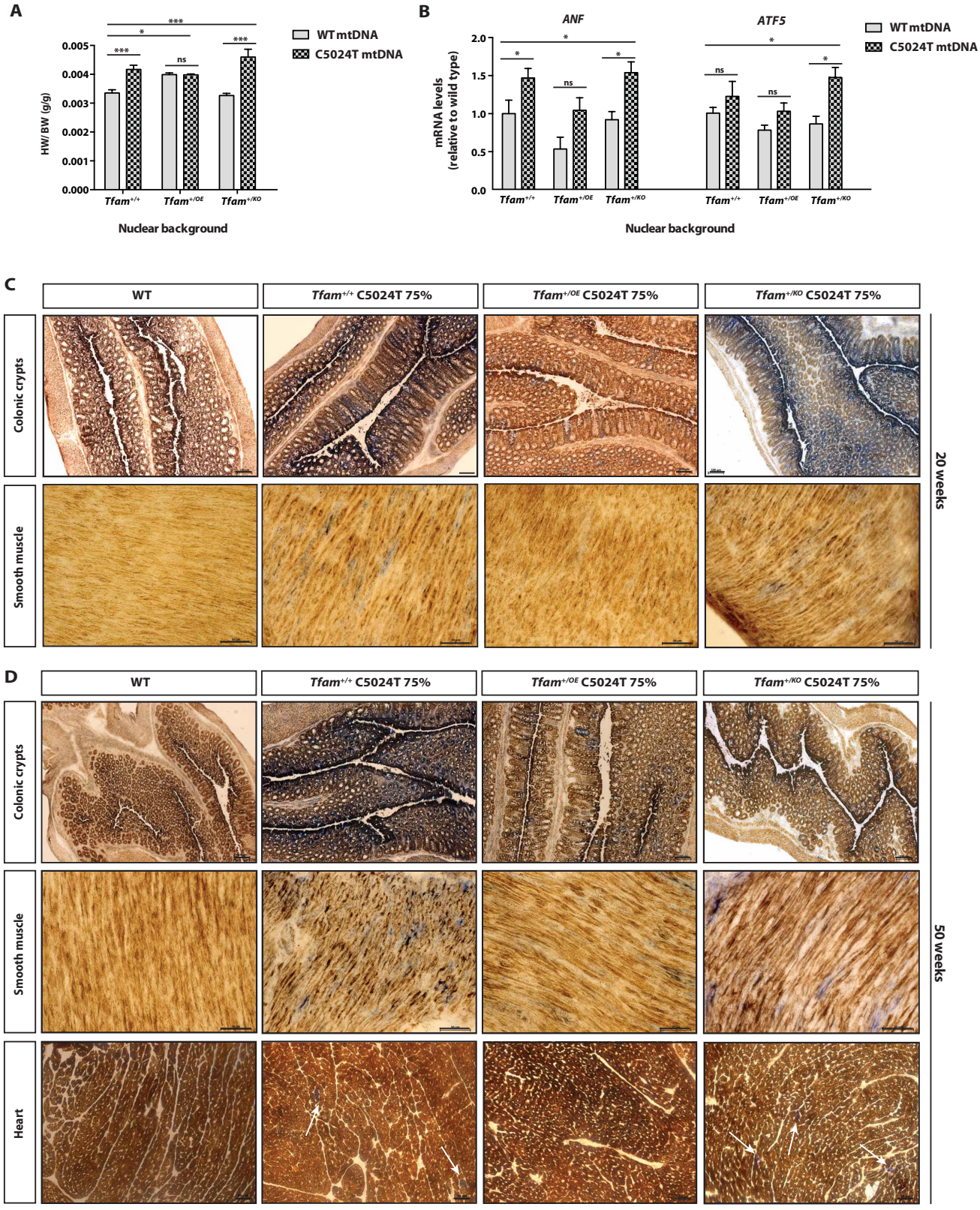

Fig. 2. Different levels of mtDNA modulate the phenotypic manifestations of the C5024T mutation. (**A**) The ratio of heart (HW) to body weight (BW) (g/g) in males at 50 weeks of age. (**B**) *ANF* and *ATF5* expression levels as measured by qPCR at 50 weeks of age. Data are represented as means ± SEM; **P* < 0.05; ****P* < 0.001; *n* > 5. (**C** to **D**) Representative COX/SDH staining of colonic crypts and smooth muscle at 20 weeks of age (C) and of colonic crypts, smooth muscle, and heart at 50 weeks of age (D) from mice with WT or C5024T mtDNA combined with the *Tfam*$^{+/+}$, *Tfam*$^{+/OE}$, or the *Tfam*$^{+/KO}$ alleles. Scale bars, 100 μm (colonic crypt) 50 μm (heart and smooth muscle).

50- to 75-week-old animals with WT mtDNA harboring the $Tfam^{+/+}$, $Tfam^{+/OE}$, or $Tfam^{+/KO}$ alleles (fig. S2A), consistent with our previous reports that moderately increased or reduced TFAM expression does not affect respiratory chain function (*19*, *20*). In contrast, C5024T animals with high mutation levels showed a prominent impairment of COX activity in colonic epithelium and smooth muscle at 20 and 50 weeks of age (Fig. 2, C and D). Overexpression of TFAM in C5024T animals with high mutation levels significantly reduced the extent of COX deficiency in colonic epithelium and smooth muscle (Fig. 2, C and D, and fig. S2, C and D). Unexpectedly, decreased mtDNA levels had tissue-specific effects on the phenotype. The $Tfam^{+/KO}$ C5024T animals showed a similar or a more profound respiratory chain dysfunction in smooth muscle in comparison with C5024T mice at 20 and 50 weeks of age (Fig. 2, C and D, and fig. S2, B and C). In contrast, there were marked changes with age in the severity of COX deficiency in colonic epithelium. In $Tfam^{+/KO}$ C5024T animals, the number of COX-deficient colonic crypts was unchanged at the age of 20 weeks (Fig. 2C and fig. S2D), whereas deficient colonic crypts were much less abundant at the age of 50 weeks (Fig. 2D and fig. S2D).

Only very few COX-deficient cardiomyocytes (Fig. 2D, white arrows) were present in hearts from C5024T mice. COX-deficient cardiomyocytes were present at an even lower frequency in $Tfam^{+/OE}$ C5024T mice, whereas they became slightly more abundant in $Tfam^{+/KO}$ C5024T animals (Fig. 2D). In skeletal muscle, COX-deficient cells were very rare, and their frequency was not affected by alterations in mtDNA levels, even at 75 weeks of age (fig. S2E). Our findings thus show that increased mtDNA copy number can markedly ameliorate OXPHOS phenotypes in different tissues of C5024T mice.

The mtDNA copy number influences the steady-state levels of $tRNA^{Ala}$ and mitochondrial function

To elucidate whether the improvement of phenotypes was accompanied by increased mitochondrial translation, we performed a set of molecular analyses. It should be noted that pathogenic tRNA mutations typically cause a mosaic OXPHOS deficiency in affected tissues, consistent with what we show here (Fig. 2), and molecular analyses of tissue homogenates therefore often reveal only modest changes despite markedly affected function in individual cells (*22*). Northern blot and qPCR analyses of steady-state levels of mitochondrial tRNAs and mRNAs in the heart and colon of C5024T mice at 50 weeks of age showed a substantial depletion of $tRNA^{Ala}$ (Fig. 3, A and B), whereas the levels of the other mtDNA-encoded transcripts were slightly increased or unchanged (fig. S3, A to C).

In colon of mice with WT mtDNA, the $Tfam^{+/OE}$ genotype caused increased steady-state levels of $tRNA^{Ala}$, whereas the $Tfam^{+/KO}$ genotype had no clear impact (Fig. 3, A and B). In colon of C5024T mice, up- or down-regulation of TFAM expression had no significant effect on the decreased steady-state levels of $tRNA^{Ala}$ (Fig. 3, A and B). The explanation for this finding is likely that there are competing processes in colonic tissue in C5024T mice, with an increase of COX-deficient smooth muscle cells (fig. S2C), whereas the epithelium of the colonic crypts shows a decline of COX-deficient cells with time (fig. S2D).

In hearts with WT mtDNA, the $Tfam^{+/OE}$ and $Tfam^{+/KO}$ genotype did not lead to changes in $tRNA^{Ala}$ levels in comparison with $Tfam^{+/+}$ animals (Fig. 3B). In contrast, in hearts of C5024T mice, the $Tfam^{+/OE}$ genotype led to a moderate increase of $tRNA^{Ala}$ levels, while the $Tfam^{+/KO}$ genotype led to a further reduction of tRNA levels (Fig. 3, A and B).

We proceeded with translation assays in isolated mitochondria from colon of 50-week-old animals harboring the C5024T mutation and found a marked decrease of in organello translation (Fig. 3C). Modulation of TFAM expression had no effect or only slightly ameliorated the translation defect (Fig. 3C). We also analyzed in organello translation in isolated heart mitochondria in 50-week-old C5024T mice and found impaired mitochondrial protein synthesis (Fig. 3C), in line with our previous results (*15*). Overexpression of TFAM partially reversed the impaired translation in heart mitochondria, whereas reduced TFAM expression enhanced the translation defect (Fig. 3C).

As the C5024T mutation leads to a robust decrease in de novo mitochondrial protein synthesis, we decided to analyze the steady-state levels of some OXPHOS subunits and the activity of respiratory chain complexes in mitochondrial extracts from heart and colon of mice harboring the C5024T mutation. Despite decreased mitochondrial translation, the steady-state levels of the analyzed proteins showed minor alterations and only when the TFAM expression was decreased (fig. S3D). In colon of $Tfam^{+/KO}$ C5024T animals at 50 weeks of age, the steady-state levels of complex III (CIII) and CV subunits were slightly increased; whereas in the heart, the levels of components of CI, CII, and CIII were decreased (fig. S3D). We also measured the activities of respiratory chain complexes (Fig. 3D) at 50 weeks of age. The C5024T mice exhibited a moderate, although not significant, impairment in CI, CI + CIII, and CIV activities in colon (~80 to 90% of WT controls), whereas no clear effects were observed in the heart. The increased TFAM expression completely reversed the mild biochemical defects in colon. In contrast, reduced TFAM expression decreased the CI, CI + CIII, CII + CIII enzyme activities in the heart and the CI and CI + CIII enzyme activities in colon. Here, we show that increasing mtDNA copy number has beneficial effects on the pathology associated with the C5024T mutation, whereas reduced mtDNA copy number has tissue-specific effects.

The mtDNA copy number affects the level of heteroplasmy in proliferating tissues

The unexpected observation of a clear tissue-specific difference in the pattern of OXPHOS dysfunction in colon and heart (Figs. 2 and 3) suggests that the extent of cell proliferation may be an important determinant of the phenotype. We therefore measured the mutation levels in postmitotic and proliferative tissues of C5024T mice at the ages of 20, 50, and 75 weeks (Fig. 4, A to C). The mutation levels in ear clips at the age of 3 weeks were very similar to the levels in tail, heart, and quadriceps muscle at the age of 75 weeks (Fig. 4C). In contrast, the mutation levels in colon and small intestine at this age were substantially lower than the levels in ear clips (Fig. 4C), consistent with negative selection against mutated mtDNA in these tissues during adult life (*16*). Selection against the C5024T mtDNA was observed from 20 weeks of age in the small intestine and from 50 weeks in colon (Fig. 4, A and B). In both tissues, the levels of mutated mtDNA decreased with increasing age. Increased mtDNA copy number did not affect heteroplasmy levels, whereas decreased mtDNA copy number led to an earlier onset and more pronounced selection against mutated mtDNA (Fig. 4, A to C). A detailed comparison of temporal changes of C5024T mutation levels in the heart, containing mainly postmitotic cells, and the colon, containing a large amount of rapidly dividing cells, illustrates the tissue-specific differences (Fig. 4, D to F). The C5024T mice have similar mutation levels at the

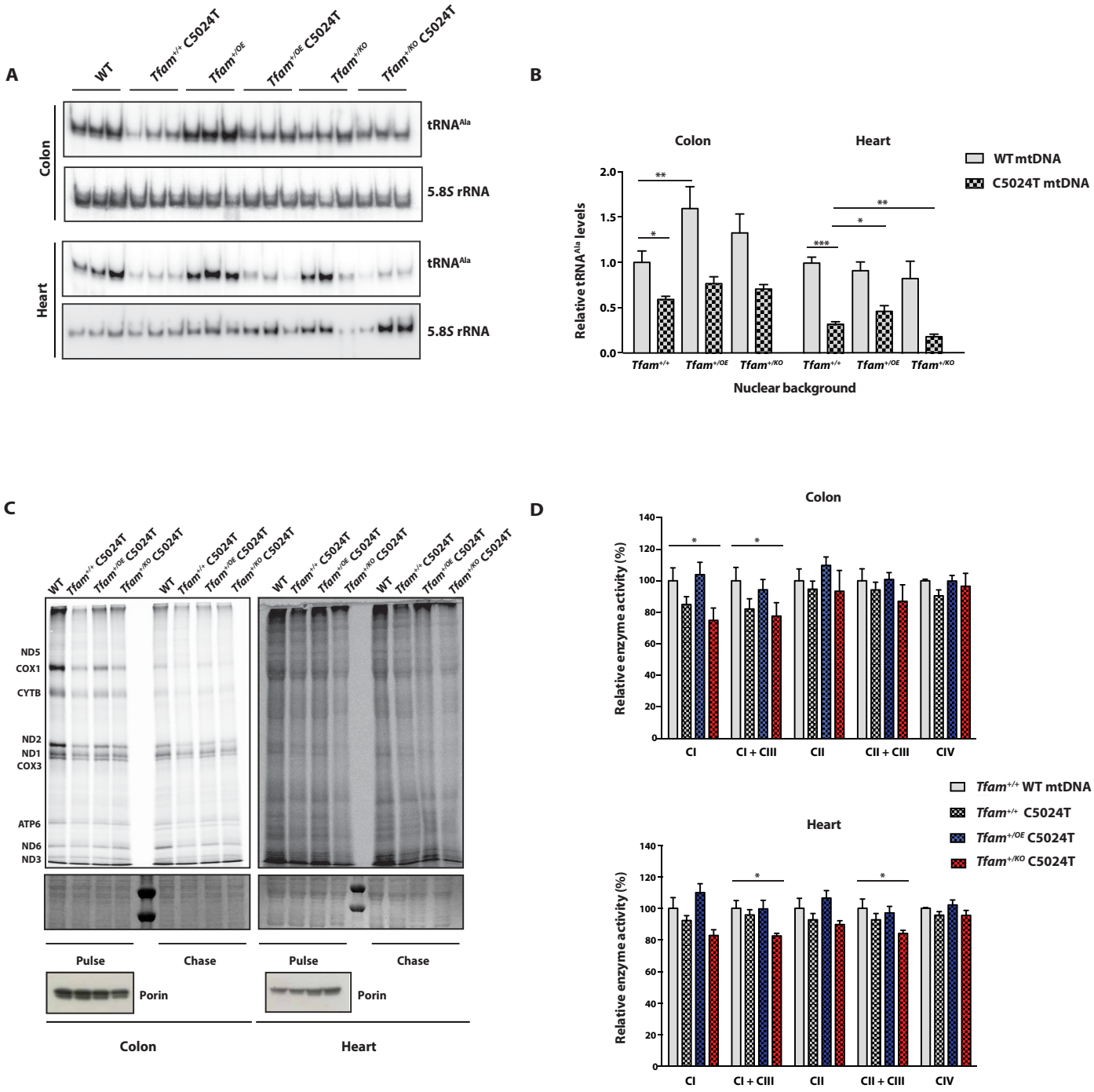

Fig. 3. Levels of mtDNA modulate tRNA^{Ala} expression, mitochondrial translation, and OXPHOS function. All analyses were performed in heart and colon of C5024T mice at 50 weeks of age. (**A**) Representative Northern blot analysis of mitochondrial tRNA^{Ala} and nuclear 5.8*S* rRNA (as loading control) levels. (**B**) Quantification of the steady-state levels of tRNA^{Ala}. (**C**) Representative in organello translation assays of mitochondria isolated from colon and heart. Coomassie staining and Western blot analysis of porin are shown as loading controls. CYTB, cytochrome b. (**D**) Respiratory chain enzyme activity assays of CI, CI + CIII, CII, CII + CIII, and CIV in mitochondrial protein extracts from heart and colon. Data are represented as means ± SEM; **P* < 0.05; ***P* < 0.01; ****P* < 0.001; *n* > 5.

age of 20 weeks in the heart and colon, but with increasing age, there is a significant selection against mutated mtDNA in colon (Fig. 4D). Reduced TFAM expression markedly enhanced the selection against mutated mtDNA in colon (Fig. 4F).

Increased mtDNA copy number does not affect the mutation load in colonic crypts

To further explore why reduced mtDNA copy number has a strong impact on selection against mutated mtDNA in the colon, the most

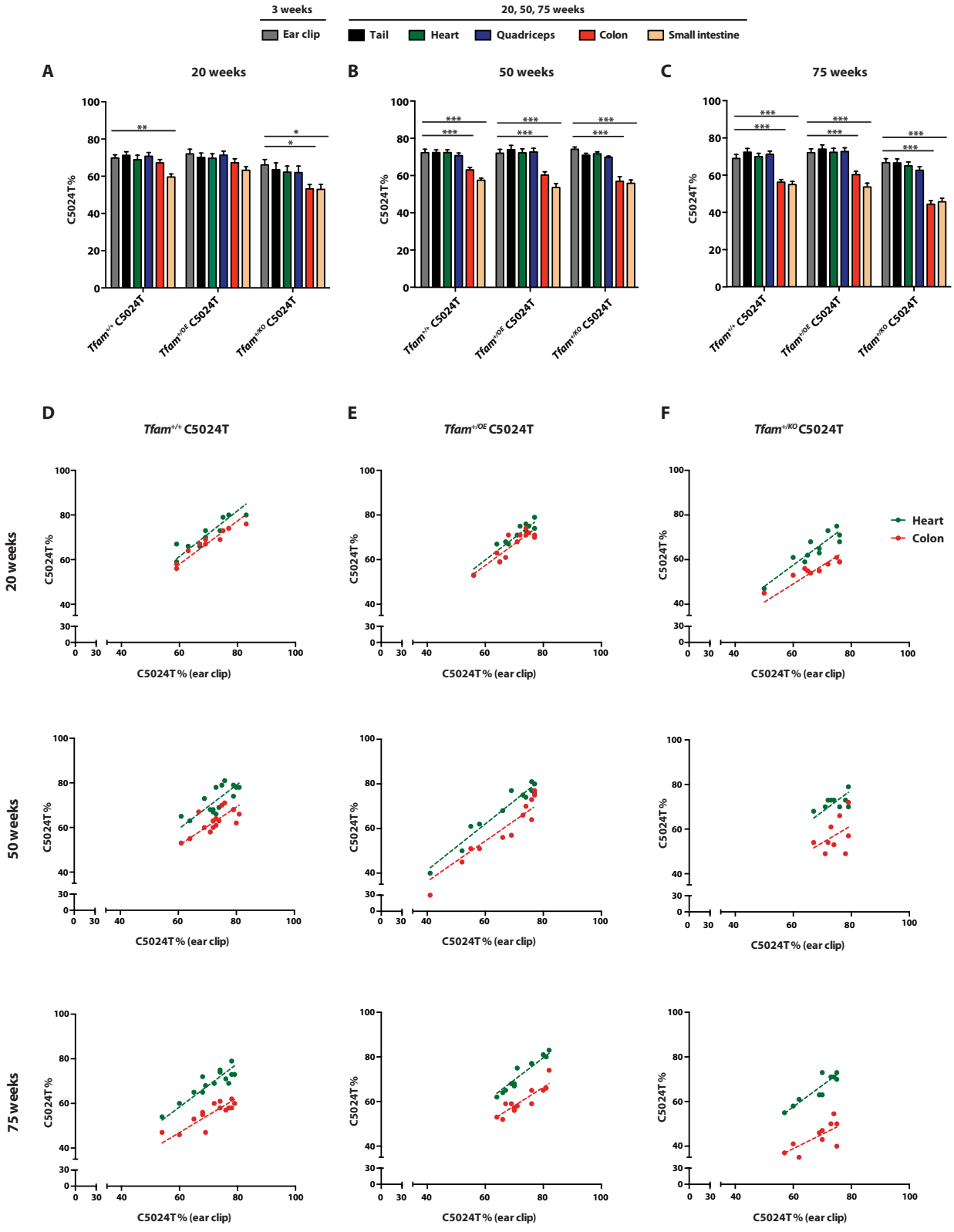

Fig. 4. The mtDNA copy number regulates the segregation of the C5024T mutation in proliferating tissues of aged mice. (**A** to **C**) Relative levels of the C5024T mutation were measured with pyrosequencing. The mutation levels in an ear clip at 3 weeks of age was compared with mutation levels in the tail, quadriceps, muscle, heart, colon, and small intestine at 20 weeks (A), 50 weeks (B), and 75 weeks (C) of age in *Tfam*$^{+/+}$ C5024T, *Tfam*$^{+/OE}$ C5024T, and *Tfam*$^{+/KO}$ C5024T mice. Data are represented as means ± SEM; *$P < 0.05$; **$P < 0.01$; ***$P < 0.001$; $n > 10$. (**D** to **F**) Comparison between levels of heteroplasmy in heart and colon of individual mice of the genotypes *Tfam*$^{+/+}$ C5024T (D), *Tfam*$^{+/OE}$ C5024T (E), and *Tfam*$^{+/KO}$ C5024T (F) at 20, 50, and 75 weeks of age, respectively.

rapidly renewing tissue in the mammalian body (*23*), we analyzed mutation levels in individual crypts. To this end, we performed COX/SDH staining in colon at 20 and 50 weeks of age, followed by laser microdissection of individual COX-positive (COX^+, brown) and COX-negative (COX^-, blue) crypts (Fig. 5A). By measuring the levels of heteroplasmy in both young and adult C5024T mice, we observed that the COX-deficient crypts were characterized by very high levels of the C5024T mutation (around 90%), whereas the COX^+ crypts contained lower heteroplasmy levels (Fig. 5, B and C). Increased mtDNA copy number did not influence the correlation between high C5024T mutation load and COX deficiency at any age (Fig. 5, B and C). That is, in *Tfam*$^{+/OE}$ C5024T mice, the blue and brown crypts did not carry higher or lower levels of heteroplasmy in comparison with C5024T mice despite the partial rescue of COX deficiency (Fig. 2D and fig. S2D). In *Tfam*$^{+/KO}$ mice, we detected the presence of two populations of COX-deficient crypts having either high (72 to 90%) or low (7 to 43%) levels of the C5024T mutation at the age of 50 weeks (Fig. 5C), consistent with an ongoing selection against high mutation levels.

As our data show that TFAM overexpression ameliorates mitochondrial defects in colonic crypts without affecting the level of heteroplasmy, the increase of the total amount of WT mtDNA is important in determining disease phenotype severity. A higher mtDNA copy number will decrease clonal expansion of mutated mtDNA, meaning that mutation levels sufficient to impair COX activity are less likely to be reached. In contrast, when mtDNA copy number is significantly decreased, clonal expansion of mutated mtDNA will occur faster. Cells with high levels of mutated mtDNA are selected against, and this negative selection process is facilitated by the more rapid clonal expansion caused by decreased mtDNA copy number.

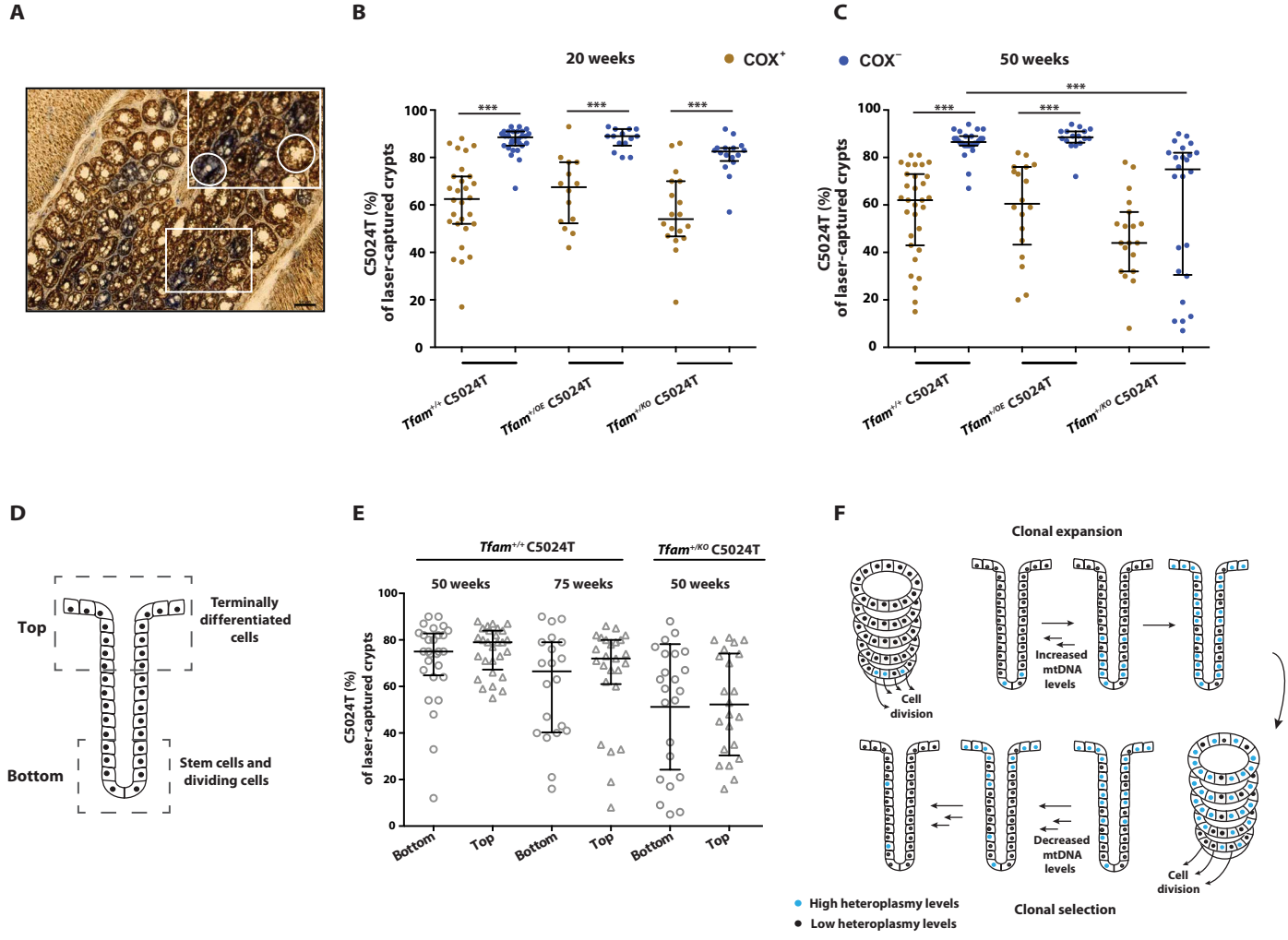

Fig. 5. The mtDNA copy number affects the levels of heteroplasmy in the colonic epithelium. (**A**) Representative COX/SDH staining of colonic epithelium. In white circles, two examples of COX^+ (brown) and COX^- (blue) crypts collected with laser capture microdissection. (**B** and **C**) Levels of heteroplasmy measured in individual laser-captured crypts from *Tfam*$^{+/+}$ C5024T, *Tfam*$^{+/OE}$ C5024T, and *Tfam*$^{+/KO}$ C5024T mice at 20 (B) and 50 (C) weeks of age. Data are represented as means ± SEM. Fifteen to 30 crypts (blue and brown) were collected from two mice for each genotype and time point; ***$P < 0.001$. (**D**) Schematic architecture of the colonic crypt. The bottom portion contains the stem cell compartment at the base of the crypt, whereas highly specialized and differentiated colon epithelial cells are localized in the upper (top) portion. (**E**) Levels of heteroplasmy measured in individual laser-captured bottom (circles) and top (triangles) segments of crypts from *Tfam*$^{+/+}$ C5024T mice at 50 and 75 weeks of age and from *Tfam*$^{+/KO}$ C5024T mice at 50 weeks of age. Data are represented as a median ± interquartile range. In total, 21 to 28 half crypts (top and bottom) were collected from two mice for each genotype and time point. (**F**) Proposed model for clonal selection against high levels of the C5024T mutation in colonic crypts.

Reduced mtDNA levels exacerbate the clonal selection in the stem cell niche of the colonic crypts

To gain insight into the process of selection against high mutation levels, we decided to investigate the distribution of the $tRNA^{Ala}$ mutation along the crypt axis in adult (50 weeks) and aged (75 weeks) C5024T mice. The crypts (Fig. 5D) are the functional unit of the colonic epithelium and contain stem cells at the base, which divide to produce the specialized cells in the upper part of the crypts (*24*). We collected the two portions (bottom and top) of longitudinal sections of COX^+ and COX^- crypts and quantified the mutation load (Fig. 5E). At 50 weeks of age, the C5024T mice had a mutation load that was very similar all along the axis of the crypts, although a few cells with very low levels of the C5024T mutation (<40%) were detected at the base of the crypts. However, at 75 weeks, cells with low levels of the C5024T mutation were more abundant at the base and were also present at the apex of the crypts (Fig. 5E). In $Tfam^{+/KO}$ C5024T mice at 50 weeks of age (Fig. 5E), the longitudinal distribution of the level of heteroplasmy resembled the one observed in 75-week-old C5024T mice, showing that decreased mtDNA levels promote an earlier onset of clonal selection. This bimodal distribution of mutated mtDNA in 50-week-old $Tfam^{+/KO}$ C5024T mice led to lower median mutation levels in both portions of the crypt (Fig. 5E). These results show that the process of clonal selection starts in the stem cell compartment in the base of the crypts and is facilitated by decreased mtDNA levels (Fig. 5F).

DISCUSSION

Many mitochondrial diseases are caused by heteroplasmic mtDNA mutations, meaning that affected patients carry a fraction of perfectly functional WT mtDNA. It has been widely recognized that most mtDNA mutations, both point mutations and deletions, are functionally recessive and therefore only cause OXPHOS deficiency if present above a certain threshold. However, the interdependency between the relative levels of heteroplasmy and the absolute amount of WT mtDNA has remained enigmatic to define. We show here that increased absolute levels of WT mtDNA can improve OXPHOS function, even if mutant mtDNA is the predominant species in the affected tissue.

At present, no effective curative treatments are available for patients with mtDNA disorders, and patient management is therefore mostly focused on ameliorating symptoms, e.g., epilepsy, heart failure, and diabetes. Many heteroplasmic pathogenic mtDNA mutations can be tolerated at very high levels, as exemplified by the A8344G mutation of $tRNA^{Lys}$ causing the myoclonus epilepsy and ragged-red fibers (MERRF) syndrome. Affected patients typically have >90% mutated mtDNA in skeletal muscle, whereas siblings carrying up to 90% of this mutation can be unaffected (*25*). A slight decrease of the mutated mtDNA fraction would thus cure patients with MERRF if treatment could be administrated before irreversible cell loss has occurred. Similar sharp thresholds have also been observed for other types of mtDNA mutations, e.g., large mtDNA deletions causing chronic progressive external ophthalmoplegia or Kearns-Sayre syndrome, and the A3243G mutation of the $tRNA^{Leu(UUR)}$ gene causing mitochondrial encephalopathy, lactic acidosis, and stroke-like episodes (MELAS) syndrome (*12*).

Over the last two decades, different approaches have been developed with the aim to manipulate the balance between WT and mutated mtDNA (*26*, *27*). Experimental studies have shown that expression of mitochondrially targeted endonucleases can efficiently digest mutated mtDNA and shift the mutation threshold in favor of WT mtDNA (*28*). Transcription activator-like effector nucleases (TALENs) and zinc finger nucleases (ZFNs) targeted to mitochondria can efficiently cleave mutated mtDNA in cell lines (*29*, *30*). Recently, preclinical proof of concept for this treatment strategy has been obtained in a mouse model harboring the same pathogenic C5024T $tRNA^{Ala}$ mutation as we used in this study. The C5024T mice were treated with mitochondrially targeted TALENs (*31*) or mitochondrially targeted ZFNs (*32*) delivered by intravenous injection of adeno-associated virus (AAV). In principle, these treatments are capable of targeting a wide variety of mtDNA mutations but are limited by the requirement to define a suitable recognition sequence for the endonuclease. Moreover, the large size, especially of the TALEN endonucleases, makes packaging into virus particles challenging. Furthermore, the AAV approach suffers from the same limitations as gene therapy approaches in general: The treatment procedure is laborious and expensive, and strategies still need to be developed for efficient targeting of affected cell types in the central nervous system.

As an alternative to destroying mutated mtDNA, a general stimulation of mitochondrial biogenesis has been proposed. Experiments in the mouse have shown that increasing the overall amount of malfunctioning mitochondria in skeletal muscle has beneficial effects as the overall ATP production will increase, although the individual mitochondria have severely impaired function (*33*). Hence, stimulation of mitochondrial biogenesis by the activation of transcriptional peroxisome proliferator–activated receptor-γ coactivator 1α (PGC1-α) has been used as a treatment strategy for mitochondrial myopathy (*34*). The pan-PPAR (pan-peroxisome proliferator-activated receptor) agonist bezafibrate or the AMP-activated protein kinase agonist AICAR (5-aminoimidazole-4-carboxamide ribonucleotide) has been reported to activate PGC1-α, but problems with reproducing preclinical results and unwarranted complications have dampened the enthusiasm. Moreover, the efficiency of this approach may depend on the affected tissues, e.g., skeletal muscle has a large capacity to induce mitochondrial biogenesis, whereas other tissues may have a much more limited capacity. Last, it should be pointed out that transcription activators and coactivators frequently influence several intracellular processes and are therefore unlikely to selectively increase OXPHOS without affecting a variety of other metabolic pathways.

We have previously shown that the infertility phenotype in the mtDNA mutator mice, which carries a large number of different point mutations of mtDNA and a linear deletion (*35*, *36*), can be, at least, partly reversed by increasing total mtDNA copy number (*21*). Although this model has been extensively used for studies of the role for mitochondrial dysfunction in aging (*37*), the complex clinical and genetic phenotype makes it impractical for studies of mechanisms relevant for human mitochondrial disease caused by single mtDNA mutations.

Clinical studies indicate that mtDNA copy number has a role in the pathology of mitochondrial diseases caused by mtDNA mutations. Patients affected by mitochondrial myopathy have been reported to have a progressive loss of WT mtDNA (*38*). Levels of mtDNA have also been described as an important factor that distinguishes asymptomatic carriers from patients affected with Leber hereditary optic neuropathy (*14*). Moreover, mtDNA copy number was recently associated with disease severity and progression in skeletal muscle of patients with MELAS (*39*). Although patients with high levels of heteroplasmy tend to have severe clinical phenotypes, the proportion of the mutant allele is not the sole determinant of the genotype-phenotype correlation of mitochondrial disease (*40*), and

mtDNA copy number is one of several other plausible explanations for the intra-individual variation influencing the clinical outcome.

An increase of total mtDNA levels concomitantly with unaltered levels of heteroplasmy raises the absolute amount of both WT and mutated mtDNA in C5024T mice. We show here that an increased gene dosage of WT mtDNA has a major impact on ameliorating OXPHOS function despite that mutated mtDNA is the most abundant genome. Unexpectedly, a reduction in mtDNA copy number also has beneficial effects in certain tissues, such as the colonic crypts, because it facilitates clonal expansion and selection against mutated mtDNA, which, in turn, results in improved OXPHOS function with time. Clonal expansion of mtDNA mutations in colonic crypts also occurs in aging mice and humans (*41*) because mtDNA mutations accumulate in the stem cell niche of colonic crypts as consequence of relaxed replication and/or somatic segregation (*42*). Over time, the continual division of stem cells favors the expansion of cells with a lower mutation load (clonal selection), and these cells will repopulate the entire crypt, as has recently been suggested to occur in colonic epithelium in patients with MELAS and MERFF (*43*). A similar process of selection has also been observed in human patients with MELAS where the levels of the A3243G mutation decrease with age in blood (*13*), consistent with loss of hematopoietic stem cells with high mutation levels (*44*). On the basis of the results we present here, we propose a model whereby the mtDNA levels influence the selection against heteroplasmic mtDNA mutations in colonic stem cells (Fig. 5F). Our data show that an increased amount of WT mtDNA decreases the clonal expansion of the C5024T mutation, whereas decreased mtDNA copy number accelerates clonal selection against mutated mtDNA in the stem cell niche (Fig. 5F).

To summarize, our results provide experimental in vivo evidence that modulation of mtDNA copy number represents a potential therapeutic approach for the treatment of mitochondrial diseases caused by pathogenic mutations in mtDNA. Although the mechanism regulating mtDNA maintenance and copy number is incompletely understood (*45*), the experimental data presented here confirm the key role of TFAM in this process. Pharmacological or gene therapy approaches to increase TFAM levels may thus provide a future avenue for treatment of mitochondrial disease.

MATERIALS AND METHODS

Study design

This study aimed to elucidate the impact of mtDNA copy number on the pathology caused by the heteroplasmic mtDNA C5024T mutation. To this end, we genetically manipulated the mtDNA levels in C5024T mice and then analyzed the effect on the phenotype at different disease stages (20, 50, and 75 weeks of age). Mitochondrial function was evaluated using (i) histochemistry and enzymatic assay to test OXPHOS activity, (ii) Northern blot and qPCR analyses to measure steady-state levels of mtDNA-encoded transcritps, and (iii) in organello translation and Western blot analyses to estimate the mitochondrial protein synthesis. The mitochondrial genome was analyzed in terms of mtDNA copy number by qPCR and the level of heteroplasmy by pyrosequencing. All experiments were performed on in vivo tissues and, unless otherwise specified, data were collected from at least five mice for each genotype and for each time point to achieve consistent results and to evaluate significant differences between groups. The investigators were blinded when conducting histochemistry and the quantification of COX-deficient cells in the colonic epithelium and smooth muscle.

Mouse models

Mice harboring $tRNA^{Ala}$ (C5024T) (*15*), Tfam BAC ($Tfam^{+/OE}$) (*21*), and $Tfam^{+/KO}$ (*19*) were generated as previously described. Mice used in all experiments had an inbred C57BL/6NCrl nuclear background (strain code 027; Charles River Laboratories, Germany). Animals were housed in a 12-hour light/dark cycle at 21°C and fed ad libitum on a standard mouse food (ssniff RM-H Low-Phytoestrogen) or an enhanced diet during breeding and for newly weaned mice (ssniff M-Z Low-Phytoestrogen) from Ssniff Spezialdiaeten GmbH. The study was approved by the Landesamt für Natur, Umwelt und Verbraucherschutz Nordrhein–Westfalen and performed in accordance with the recommendations and guidelines of the Federation of European Laboratory Animal Science Associations.

DNA isolation and mtDNA quantification

Genomic DNA from snap-frozen heart and colon was isolated using the DNeasy Blood and Tissue Kit (Qiagen), following the manufacturer's instructions. Quantification of mtDNA copy number was performed in triplicates using 5 ng of DNA using TaqMan Universal Master Mix II and TaqMan probes from Life Technologies. The mtDNA levels were assessed using probes against the mitochondrial genes (ND1 and ND6), and nuclear 18*S* rRNA served as a loading control.

Quantification of the C5024T mutation levels

Relative levels of the mutant and WT mtDNAs were quantified using a PyroMark Q24 pyrosequencer (Qiagen) (*15*). Briefly, this assay was developed using PyroMark assay design software v2.0 (Qiagen). A PCR reaction was performed to amplify a 178–base pair fragment containing the C5024T mutation site using a biotinylated forward primer and a nonbiotinylated reverse primer. After adding a PyroMark binding buffer (Qiagen) and 1 μl Streptavidin Sepharose TM high-performance beads (GE Healthcare), PCR products were purified and denaturated using a Pyromark Q24 vacuum workstation (Qiagen). Sequencing was carried out with PyroMark Gold Q24 Reagents according to manufacturer's directions, using specific gene-sequencing primers 5′Biotin TTCCACCCTAGCTATCATAAGC (forward) and GTAGGTTTAATTCCTGCCAATCT (reverse) and the sequencing primer TGTAGGATGAAGTCTTACA.

Western blot

Isolation of mitochondria from mouse heart and colon was performed by differential centrifugation (*46*). Twenty micrograms of isolated mitochondria or 50 μg of total protein extracts was resuspended in 4× Laemmli buffer. Proteins were separated by SDS–polyacrylamide gel electrophoresis (PAGE) using 12% precast gels (Invitrogen) and then transferred onto polyvinylidene difluoride membranes (GE Healthcare). Immunodetection was performed according to standard techniques using enhanced chemiluminescence Immun-Star HRP Luminol/Enhancer (Bio-Rad). The following antibodies were used: SDHA (ab14715, Abcam), Ndufs3 (ab14711, Abcam), VDAC/Porin (ab128568, Abcam), ATP synthase subunit alpha (Molecular Probes A21350, Thermo Fisher Scientific), UQCRC1 CIII subunit core1 (Molecular Probes A21362, Thermo Fisher Scientific), COX I (459600, Invitrogen), TFAM (rabbit polyclonal antisera against TFAM generated using recombinant mouse protein), and GAPDH (ab8245, Abcam).

Tissue preparation

Mice were euthanized with CO_2. Tissues were collected and washed with phosphate-buffered saline (PBS) to remove remaining blood or feces. Tissues used for COX/SDH staining were frozen in isopentane (15 s) that was previously cooled to −160°C in liquid nitrogen. Tissues used in other analyses were snap-frozen in liquid nitrogen. Tissues were cryosectioned at −12°C (14 μm for colon and quadriceps, 10 μm for heart; Thermo Scientific Microm HM560). The sections used for histochemistry were cut on permanent coated slides (VWR) and the sections for laser capture dissection (14 μm) on to polyethylenenaphthalate (PEN) slides (Leica Microsystems). Both types of sections were stored at −80°C before further analysis.

Dual COX/SDH enzyme histochemistry

Sections were incubated in freshly prepared COX medium [100 μM cytochrome *c*, 4 mM diaminobenzidine tetrahydrochloride, catalase (20 μg/ml), and 0.2 M phosphate buffer (pH 7.0)]. After incubation for 45 min at 37°C, slides were washed three times in PBS. Thereafter, slides were incubated in freshly prepared SDH medium [130 mM sodium succinate, 200 μM phenazinemethosulphate, 1 mM sodium azide, 1.5 mM nitroblue tetrazolium, and 0.2 M phosphate buffer (pH 7.0)] for 30 min for colon and quadriceps and 10 min for heart at 37°C. Last, slides were washed three times with PBS, dehydrated (following concentration of ethanol: 70%, 75%, 95%, and 2× 99.5%) and mounted for bright-field microscopy. The sections for laser capture dissection (14 μm) were similarly exposed to COX/SDH staining, dehydrated, and air-dried for 60 min.

RNA isolation and quantitative reverse transcription PCR

Total RNA from snap-frozen heart and colon was isolated, using the ToTALLY RNA kit (Ambion) and quantified with a Qubit fluorometer (Life Technologies). After deoxyribonuclease treatment, reverse transcription was performed using the High-Capacity cDNA Reverse Transcription Kit (Applied Biosystems, Life Technologies). qPCR was performed using the TaqMan Universal Master Mix II with TaqMan probes (*ANF*, *ATF5*, *ATF4*, *Cox1*, *Cox2*, *Nd6*, and β-*actin*) from Life Technologies. β-Actin was used as loading control.

Northern blot analysis

Steady-state levels of mitochondrial tRNAs were determined by Northern blot analysis, using 1 to 3 μg of total RNA from heart and colon. The tRNAs were separated by neutral 10% PAGE, transferred to Hybond-N+ membranes (GE Healthcare) and hybridized with [^{32}P]-labeled probes. DNA probes were radiolabeled with an [α-^{32}P]-dCTP using the Prime-It II random primer labeling kit (Agilent). For detection of tRNAs, oligonucleotides were labeled with [γ-^{32}P]-ATP at the 5′ end using T4 polynucleotide kinase (New England Biolabs). Cytosolic 5.8*S* rRNA was used as loading control.

In organello translation

Mitochondria were isolated from fresh heart and colon by differential centrifugation. One milligram of purified mitochondria was incubated at 37°C in translation buffer [100 mM mannitol, 10 mM sodium succinate, 80 mM KCl, 5 mM MgCl2, 1 mM KH_2PO_4, 25 mM Hepes, 200 mM ATP, 5 mM guanosine 5′-triphosphate, 200 mM creatine phosphate, 6 mM creatine kinase, and cycloheximide (200 mg/ml) with 6 mg/ml of every amino acid except methionine] and 300 μCi 35S-labeled methionine for 1 hour at 37°C. For chase experiments, 500 μg of mitochondria was incubated for 2 hours at 37°C in translation buffer with cold methionine (60 μg/ml). Next, pulse and chase samples were washed in translation buffer and resuspended into Laemmli buffer [125 mM tris (pH 6.8), 4% SDS, 20% glycerol, 1.4 M 2-mercapto-ethanol, and 0.025% bromophenol blue]. The mitochondrial proteins were resolved on a 17% SDS-PAGE gel and analyzed by autoradiography. Equal loading of mitochondria was controlled by Coomassie staining and porin immunoblot.

Biochemical evaluation of respiratory chain function

Respiratory chain enzyme activities were determined on isolated mitochondria, as previously described (*47*).

Laser capture microdissection

Following COX/SDH staining, COX^+ and COX^- colonic crypts were dissected into single tubes using a Leica Microsystems LMD 7000 laser microdissection microscope (*15*). Whole or half crypts were settled to the bottom of the tube by centrifugation at 7000*g* for 10 min at 4°C. DNA was extracted in 12 μl of lysis buffer [50 mM tris-HCl (pH 8.5), 1% Tween 20, and proteinase K (20 mg/ml)] for at least 4 hours at 55°C, with a heat inactivation step at 95°C for 10 min (*42*). The extracted DNA was used directly in PCR reactions for mutation level quantification.

Statistical analysis

All statistical analyses were performed, and graphs were drawn with GraphPad Prism v6 software. All data are presented as means ± SEM (or median ± interquartile range), and unless otherwise specified, data were collected from at least five mice for each genotype. With the exception of the data concerning the germ line and the smooth muscle COX deficiency, statistical comparisons were performed using one-way analysis of variance (ANOVA), and post hoc analysis was conducted with Bonferroni multiple comparisons test. The analysis of the germ line has been performed using both Mann-Whitney test and Kolmogorov-Smirnov test. Comparisons were performed between the mutation levels in offspring born to mothers carrying similar levels of the C5024T mutation in combination with different *Tfam* gene dosages ($Tfam^{+/+}$, $Tfam^{+/OE}$, and $Tfam^{+/KO}$). Comparisons between the COX deficiency (percent severity index) in smooth muscle of 20- and 50-week-old mice were performed using χ^2 test. The number of animals (*n*) used for each experiment is indicated in the figure legends. Values of $P < 0.05$ were considered statistically significant.

SUPPLEMENTARY MATERIALS

Supplementary material for this article is available at http://advances.sciencemag.org/cgi/content/full/5/4/eaav9824/DC1

Fig. S1. Modulation of mtDNA levels in adult $Tfam^{+/+}$ C5024T mice.

Fig. S2. Tissue-specific effects of manipulation of mtDNA levels in WT and C5024T mice.

Fig. S3. The copy number of mtDNA has a minor impact on the steady-state levels of OXPHOS subunits but does not influence the steady-state levels of mtDNA-encoded transcripts.

REFERENCES AND NOTES

1. S. E. Calvo, K. R. Clauser, V. K. Mootha, MitoCarta2.0: An updated inventory of mammalian mitochondrial proteins. *Nucleic Acids Res.* **44**, D1251–D1257 (2016).
2. P. F. Chinnery, G. Hudson, Mitochondrial genetics. *Br. Med. Bull.* **106**, 135–159 (2013).
3. M. Morgenstern, S. B. Stiller, P. Lübbert, C. D. Peikert, S. Dannenmaier, F. Drepper, U. Weill, P. Höß, R. Feuerstein, M. Gebert, M. Bohnert, M. van der Laan, M. Schuldiner, C. Schütze, S. Oeljeklaus, N. Pfanner, N. Wiedemann, B. Warscheid, Definition of a high-confidence mitochondrial proteome at quantitative scale. *Cell Rep.* **19**, 2836–2852 (2017).
4. H. A. L. Tuppen, E. L. Blakely, D. M. Turnbull, R. W. Taylor, Mitochondrial DNA mutations and human disease. *Biochim. Biophys. Acta* **1797**, 113–128 (2010).

5. G. S. Gorman, P. F. Chinnery, S. DiMauro, M. Hirano, Y. Koga, R. McFarland, A. Suomalainen, D. R. Thorburn, M. Zeviani, D. M. Turnbull, Mitochondrial diseases. *Nat. Rev. Dis. Primers.* **2**, 16080 (2016).
6. S. Srivastava, The Mitochondrial basis of aging and age-related disorders. *Genes* **8**, 398 (2017).
7. G. Pfeffer, R. Horvath, T. Klopstock, V. K. Mootha, A. Suomalainen, S. Koene, M. Hirano, M. Zeviani, L. A. Bindoff, P. Yu-Wai-Man, M. Hanna, V. Carelli, R. McFarland, K. Majamaa, D. M. Turnbull, J. Smeitink, P. F. Chinnery, New treatments for mitochondrial disease-no time to drop our standards. *Nat. Rev. Neurol.* **9**, 474–481 (2013).
8. P. F. Chinnery, M. A. Johnson, T. M. Wardell, R. Singh-Kler, C. Hayes, D. T. Brown, R. W. Taylor, L. A. Bindoff, D. M. Turnbull, The epidemiology of pathogenic mitochondrial DNA mutations. *Ann. Neurol.* **48**, 188–193 (2000).
9. L. L. Clay Montier, J. J. Deng, Y. Bai, Number matters: Control of mammalian mitochondrial DNA copy number. *J. Genet. Genomics* **36**, 125–131 (2009).
10. J. B. Stewart, P. F. Chinnery, The dynamics of mitochondrial DNA heteroplasmy: Implications for human health and disease. *Nat. Rev. Genet.* **16**, 530–542 (2015).
11. C. Macmillan, B. Lach, E. A. Shoubridge, Variable distribution of mutant mitochondrial DNAs (tRNA(Leu[3243])) in tissues of symptomatic relatives with MELAS: The role of mitotic segregation. *Neurology* **43**, 1586–1590 (1993).
12. N. G. Larsson, D. A. Clayton, Molecular genetic aspects of human mitochondrial disorders. *Annu. Rev. Genet.* **29**, 151–178 (1995).
13. S. Rahman, J. Poulton, D. Marchington, A. Suomalainen, Decrease of 3243 A→G mtDNA mutation from blood in MELAS syndrome: A longitudinal study. *Am. J. Hum. Genet.* **68**, 238–240 (2001).
14. C. Giordano, L. Iommarini, L. Giordano, A. Maresca, A. Pisano, M. L. Valentino, L. Caporali, R. Liguori, S. Deceglie, M. Roberti, F. Fanelli, F. Fracasso, F. N. Ross-Cisneros, P. D'Adamo, G. Hudson, A. Pyle, P. Yu-Wai-Man, P. F. Chinnery, M. Zeviani, S. R. Salomao, A. Berezovsky, R. Belfort Jr., D. F. Ventura, M. Moraes, M. Moraes Filho, P. Barboni, F. Sadun, A. De Negri, A. A. Sadun, A. Tancredi, M. Mancini, G. d'Amati, P. Loguercio Polosa, P. Cantatore, V. Carelli, Efficient mitochondrial biogenesis drives incomplete penetrance in Leber's hereditary optic neuropathy. *Brain* **137**, 335–353 (2014).
15. J. H. K. Kauppila, H. L. Baines, A. Bratic, M.-L. Simard, C. Freyer, A. Mourier, C. Stamp, R. Filograna, N.-G. Larsson, L. C. Greaves, J. B. Stewart, A phenotype-driven approach to generate mouse models with pathogenic mtDNA mutations causing mitochondrial disease. *Cell Rep.* **16**, 2980–2990 (2016).
16. T. I. Alam, T. Kanki, T. Muta, K. Ukaji, Y. Abe, H. Nakayama, K. Takio, N. Hamasaki, D. Kang, Human mitochondrial DNA is packaged with TFAM. *Nucleic Acids Res.* **31**, 1640–1645 (2003).
17. Y. I. Morozov, A. V. Parshin, K. Agaronyan, A. C. M. Cheung, M. Anikin, P. Cramer, D. Temiakov, A model for transcription initiation in human mitochondria. *Nucleic Acids Res.* **43**, 3726–3735 (2015).
18. T. Kanki, K. Ohgaki, M. Gaspari, C. M. Gustafsson, A. Fukuoh, N. Sasaki, N. Hamasaki, D. Kang, Architectural role of mitochondrial transcription factor A in maintenance of human mitochondrial DNA. *Mol. Cell. Biol.* **24**, 9823–9834 (2004).
19. N.-G. Larsson, J. Wang, H. Wilhelmsson, A. Oldfors, P. Rustin, M. Lewandoski, G. S. Barsh, D. A. Clayton, Mitochondrial transcription factor A is necessary for mtDNA maintance and embryogenesis in mice. *Nat. Genet.* **18**, 231–236 (1998).
20. M. I. Ekstrand, M. Falkenberg, A. Rantanen, C. B. Park, M. Gaspari, K. Hultenby, P. Rustin, C. M. Gustafsson, N.-G. Larsson, Mitochondrial transcription factor A regulates mtDNA copy number in mammals. *Hum. Mol. Genet.* **13**, 935–944 (2004).
21. M. Jiang, T. E. S. Kauppila, E. Motori, X. Li, I. Atanassov, K. Folz-Donahue, N. A. Bonekamp, S. Albarran-Gutierrez, J. B. Stewart, N.-G. Larsson, Increased total mtDNA copy number cures male infertility despite unaltered mtDNA mutation load. *Cell Metab.* **26**, 429–436.e4 (2017).
22. M. C. Rocha, J. P. Grady, A. Grünewald, A. Vincent, P. F. Dobson, R. W. Taylor, D. M. Turnbull, K. A. Rygiel, A novel immunofluorescent assay to investigate oxidative phosphorylation deficiency in mitochondrial myopathy: Understanding mechanisms and improving diagnosis. *Sci. Rep.* **5**, 15037 (2015).
23. N. Barker, M. van de Wetering, H. Clevers, The intestinal stem cell. *Genes Dev.* **22**, 1856–1864 (2008).
24. E. Fuchs, T. Chen, A matter of life and death: Self-renewal in stem cells. *EMBO Rep.* **14**, 39–48 (2013).
25. N.-G. Larsson, M. H. Tulinius, E. Holme, A. Oldfors, O. Andersen, J. Wahlström, J. Aasly, Segregation and manifestations of the mtDNA $tRNA^{Lys}$ $A{\rightarrow}G^{(8344)}$ mutation of myoclonus epilepsy and ragged-red fibers (MERRF) syndrome. *Am. J. Hum. Genet.* **51**, 1201–1212 (1992).
26. T. Taivassalo, K. Fu, T. Johns, D. Arnold, G. Karpati, E. A. Shoubridge, Gene shifting: A novel therapy for mitochondrial myopathy. *Hum. Mol. Genet.* **8**, 1047–1052 (1999).
27. S. Santra, R. W. Gilkerson, M. Davidson, E. A. Schon, Ketogenic treatment reduces deleted mitochondrial DNAs in cultured human cells. *Ann. Neurol.* **56**, 662–669 (2004).
28. F. Bruni, R. N. Lightowlers, Z. M. Chrzanowska-Lightowlers, Human mitochondrial nucleases. *FEBS J.* **284**, 1767–1777 (2017).
29. S. R. Bacman, S. L. Williams, M. Pinto, S. Peralta, C. T. Moraes, Specific elimination of mutant mitochondrial genomes in patient-derived cells by mitoTALENs. *Nat. Med.* **19**, 1111–1113 (2013).
30. P. A. Gammage, J. Rorbach, A. I. Vincent, E. J. Rebar, M. Minczuk, Mitochondrially targeted ZFNs for selective degradation of pathogenic mitochondrial genomes bearing large-scale deletions or point mutations. *EMBO Mol. Med.* **6**, 458–466 (2014).
31. S. R. Bacman, J. H. K. Kauppila, C. V. Pereira, N. Nissanka, M. Miranda, M. Pinto, S. L. Williams, N.-G. Larsson, J. B. Stewart, C. T. Moraes, MitoTALEN reduces mutant mtDNA load and restores $tRNA^{Ala}$ levels in a mouse model of heteroplasmic mtDNA mutation. *Nat. Med.* **24**, 1696–1700 (2018).
32. P. A. Gammage, C. Viscomi, M.-L. Simard, A. S. H. Costa, E. Gaude, C. A. Powell, L. Van Haute, B. J. McCann, P. Rebelo-Guiomar, R. Cerutti, L. Zhang, E. J. Rebar, M. Zeviani, C. Frezza, J. B. Stewart, M. Minczuk, Genome editing in mitochondria corrects a pathogenic mtDNA mutation in vivo. *Nat. Med.* **24**, 1691–1695 (2018).
33. A. Wredenberg, R. Wibom, H. Wilhelmsson, C. Graff, H. H. Wiener, S. J. Burden, A. Oldfors, H. Westerblad, N.-G. Larsson, Increased mitochondrial mass in mitochondrial myopathy mice. *Proc. Natl. Acad. Sci.* **99**, 15066–15071 (2002).
34. C. Viscomi, E. Bottani, G. Civiletto, R. Cerutti, M. Moggio, G. Fagiolari, E. A. Schon, C. Lamperti, M. Zeviani, In vivo correction of COX deficiency by activation of the AMPK/PGC-1α axis. *Cell Metab.* **14**, 80–90 (2011).
35. A. Trifunovic, A. Wredenberg, M. Falkenberg, J. N. Spelbrink, A. T. Rovio, C. E. Bruder, M. Bohlooly-Y, S. Gidlöf, A. Oldfors, R. Wibom, J. Törnell, H. T. Jacobs, N.-G. Larsson, Premature ageing in mice expressing defective mitochondrial DNA polymerase. *Nature* **429**, 417–423 (2004).
36. A. Ameur, J. B. Stewart, C. Freyer, E. Hagström, M. Ingman, N.-G. Larsson, U. Gyllensten, Ultra-deep sequencing of mouse mitochondrial DNA: Mutational patterns and their origins. *PLOS Genet.* **7**, e1002028 (2011).
37. D. Edgar, A. Trifunovic, The mtDNA mutator mouse: Dissecting mitochondrial involvement in aging. *Aging* **1**, 1028–1032 (2009).
38. S. E. Durham, D. T. Brown, D. M. Turnbull, P. F. Chinnery, Progressive depletion of mtDNA in mitochondrial myopathy. *Neurology* **67**, 502–504 (2006).
39. J. P. Grady, S. J. Pickett, Y. S. Ng, C. L. Alston, E. L. Blakely, S. A. Hardy, C. L. Feeney, A. A. Bright, A. M. Schaefer, G. S. Gorman, R. J. Q. McNally, R. W. Taylor, D. M. Turnbull, R. McFarland, mtDNA heteroplasmy level and copy number indicate disease burden in m.3243A>G mitochondrial disease. *EMBO Mol. Med.* **10**, e8262 (2018).
40. J. A. Morgan-Hughes, M. G. Sweeney, J. M. Cooper, S. R. Hammans, M. Brockington, A. H. V. Schapira, A. E. Harding, J. B. Clark, Mitochondrial DNA (mtDNA) diseases: Correlation of genotype to phenotype. *Biochim. Biophys. Acta* **1271**, 135–140 (1995).
41. H. L. Baines, J. B. Stewart, C. Stamp, A. Zupanic, T. B. L. Kirkwood, N.-G. Larsson, D. M. Turnbull, L. C. Greaves, Similar patterns of clonally expanded somatic mtDNA mutations in the colon of heterozygous mtDNA mutator mice and ageing humans. *Mech. Ageing Dev.* **139**, 22–30 (2014).
42. R. W. Taylor, M. J. Barron, G. M. Borthwick, A. Gospel, P. F. Chinnery, D. C. Samuels, G. A. Taylor, S. M. Plusa, S. J. Needham, L. C. Greaves, T. B. L. Kirkwood, D. M. Turnbull, Mitochondrial DNA mutations in human colonic crypt stem cells. *J. Clin. Invest.* **112**, 1351–1360 (2003).
43. T. Su, J. P. Grady, S. Afshar, S. A. McDonald, R. W. Taylor, D. M. Turnbull, L. C. Greaves, Inherited pathogenic mitochondrial DNA mutations and gastrointestinal stem cell populations. *J. Pathol.* **246**, 427–432 (2018).
44. H. K. Rajasimha, P. F. Chinnery, D. C. Samuels, Selection against pathogenic mtDNA mutations in a stem cell population leads to the loss of the 3243A→G mutation in blood. *Am. J. Hum. Genet.* **82**, 333–343 (2008).
45. N. A. Bonekamp, N.-G. Larsson, SnapShot: Mitochondrial nucleoid. *Cell* **172**, 388–388.e1 (2018).
46. A. Mourier, S. Matic, B. Ruzzenente, N.-G. Larsson, D. Milenkovic, The respiratory chain supercomplex organization is independent of COX7a2l isoforms. *Cell Metab.* **20**, 1069–1075 (2014).
47. R. Wibom, L. Hagenfeldt, U. von Döbeln, Measurement of ATP production and respiratory chain enzyme activities in mitochondria isolated from small muscle biopsy samples. *Anal. Biochem.* **311**, 139–151 (2002).

Acknowledgments: We would like to thank the Core Facility for Tissue-Based Diagnostics and Research (KI/SLL) at Karolinska University Hospital for the support provided with laser capture microdissection. We are thankful to H. Olsson for technical help. **Funding:** N.G.L. was supported by the Max Planck Society, the Novo Nordisk Foundation, the Swedish Research Council (2015-00418), and the Knut and Alice Wallenberg foundation. A.W. was supported by Ragnar Söderberg fellow in Medicine (M77/13) and the Swedish Research Council (2017-02179). **Author contributions:** R.F. performed experimental work, analyzed data, designed the experiments, and wrote the manuscript. C.K. helped to plan and supervise the

study. M.U., A.P., P.C., and R.W. helped with experimental work and data analysis. M.L.S. and J.B.S. helped with germ line data analysis. A.W. and C.F. provided scientific input. N.G.L. conceived and supervised the project and wrote the manuscript. **Competing interests:** J.B.S. and N.G.L. are inventors of the C5024T mutant $tRNA^{Ala}$ mouse, which is licensed to the pharmaceutical industry by the Max Planck Society. All other authors declare that they have no competing interests. **Data and materials availability:** All data needed to evaluate the conclusions in the paper are present in the paper and/or the Supplementary Materials. The C5024T $tRNA^{Ala}$ mutant mouse is provided by the Max Planck Society pending scientific review and a completed material transfer agreement. Requests for the C5024T $tRNA^{Ala}$ mutant mouse should be submitted to J.B.S. or N.G.L. Additional data related to this paper may be requested from the authors.

Submitted 7 November 2018
Accepted 11 February 2019
Published 3 April 2019
10.1126/sciadv.aav9824

Citation: R. Filograna, C. Koolmeister, M. Upadhyay, A. Pajak, P. Clemente, R. Wibom, M. L. Simard, A. Wredenberg, C. Freyer, J. B. Stewart, N. G. Larsson, Modulation of mtDNA copy number ameliorates the pathological consequences of a heteroplasmic mtDNA mutation in the mouse. *Sci. Adv.* **5**, eaav9824 (2019).